

Thermal and Chemical Stability of Thiol Bonding on Gold Nanostars

Mykola Borzenkov^{1,}, Giuseppe Chirico¹, Laura D'Alfonso¹, Laura Sironi¹, Maddalena Collini¹,
Elisa Cabrini², Giacomo Dacarro², Piersandro Pallavicini^{2,*}, Angelo Taglietti², Claire Bernhard³
and Franck Denat³*

¹Department of Physics “G. Occhialini”, University of Milano Bicocca, piazza della Scienza 3, 20126, Milano, Italy.

²Department of Chemistry, University of Pavia, viale Taramelli 12, 27100 Pavia, Italy.

³Institut de Chimie Moléculaire de l'Université de Bourgogne, UMR CNRS 6302, Université de Bourgogne, 21078 Dijon, France

ABSTRACT. The stability of thiol bonding on the surface of star-shaped gold nanoparticles was studied as a function of temperature in water and in a set of biologically relevant conditions. This was obtained by monitoring the release of a model fluorescent dye, Bodipy-thiol (BDP-SH), from gold nanostars (GNS) co-coated with poly(ethylene glycol) thiol (PEG-SH). The increase of the BDP-SH fluorescence emission, quenched when bound to the GNS was exploited to this purpose. A maximum 15% dye release in aqueous solution was found when the bulk temperature of gold nanostars solutions was increased to $T = 42\text{ }^{\circ}\text{C}$, the maximum physiological temperature. This fraction reduces to 3-5% for temperatures lower than $40\text{ }^{\circ}\text{C}$. Similar results were found when the temperature increase was obtained by laser irradiation on the Near Infrared (NIR) localized surface plasmon resonance (LSPR) of the GNS, that is photothermally responsive. Beside the direct impact of temperature, an increased BDP-SH release was observed changing the chemical composition of the solvent from pure water to phosphate saline buffer (PBS) and culture media solutions. Moreover, also a significant fraction of PEG-SH is released from the GNS surface due to the increase of temperature. We observed it with a different approach, *i.e.* by using a coating of α -

mercapto- ω -amino PEG labeled with Tetramethylrhodamine isothiocyanate (TRITC) on the amino group, that after heating is separated from GNS by ultracentrifugation and the released PEG determined by spectrofluorimetric techniques on the supernatant solution. These results suggest some specific limitations in the use of the gold-thiolate bond for decoration of nanomaterials with organic compounds, related to temperature and duration of the thermal treatment and of the solvent composition that could be exploited in biological media to modulate the *in vivo* release of drugs.

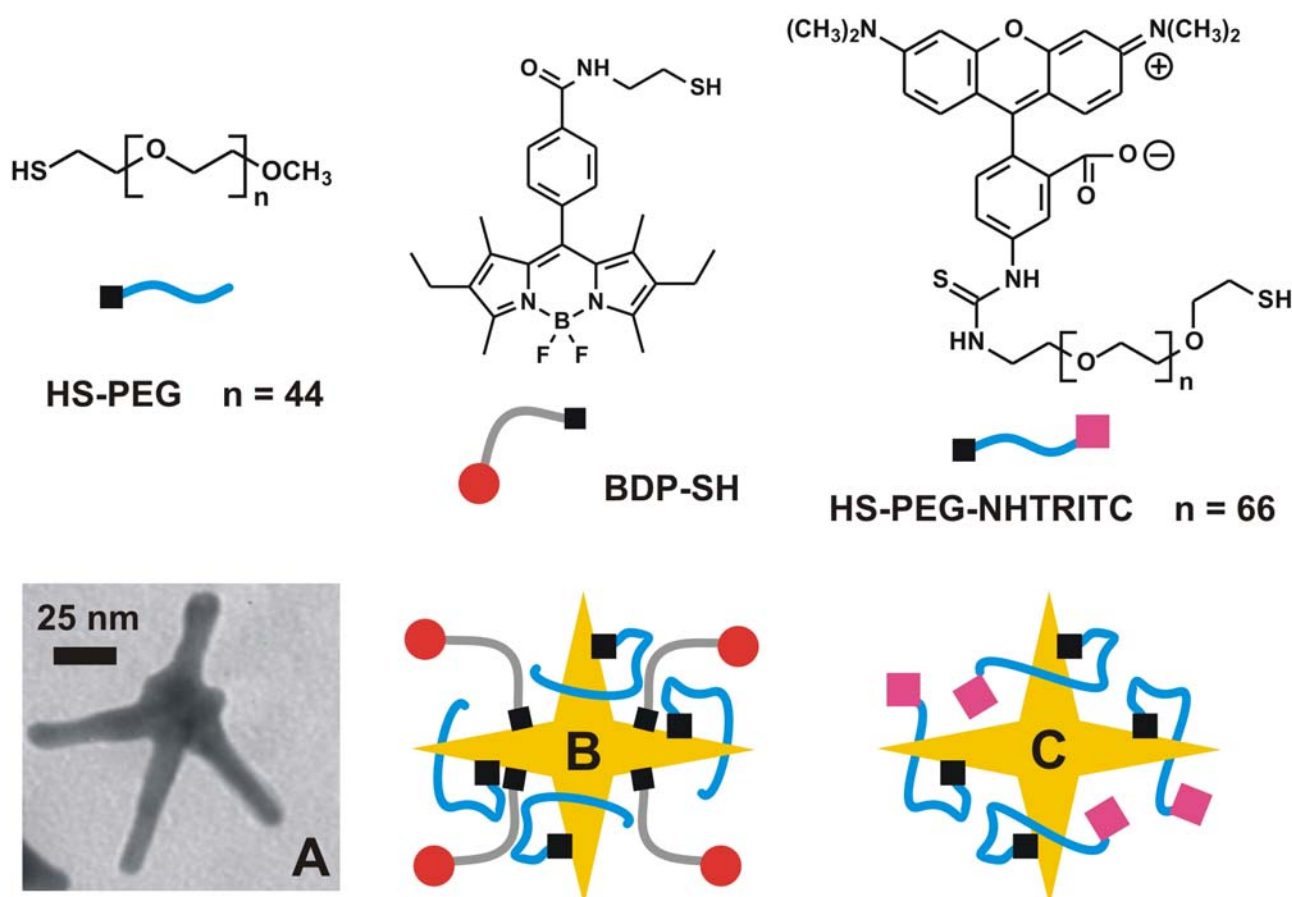
1. INTRODUCTION

Gold nanoparticles (GNP) are widely used in chemistry, physics, biology¹ and medicine² due to a number of unique properties.^{3,4} These include the light scattering and absorption from localized surface plasmon resonances^{3,5} (LSPR), whose wavelength depends mainly on the nanoparticles shape and to a lesser extent on the local dielectric constant.^{6,7} The latter is in turn tuned by the solvent and by the GNP surface coating. Besides LSPR, coating also affects GNP stability and their interaction with the environment,⁸⁻¹⁰ allowing and enriching GNP use *in vitro* and *in vivo* for bio-sensing and therapy.^{2,11-12} The direct interaction of the gold surface with thiols (-SH) and disulfides (-S-S-), forming self-assembled monolayers, is the most widely employed method for grafting a coating on GNP. This may be either a small molecule or a polymer or a combination of both.^{4,13} The formed “Au-S” bond is indeed a thiolate-Au⁺ coordinative interaction, with a homolytic strength of ~ 40 kcal/mol.^{14,15} The thermal and environmental stability of such bond has been investigated first on bulk, flat Au surfaces. Ultrahigh vacuum studies show that thiols desorb significantly from flat Au at room temperature, in a 7 days time lap.¹⁶ Desorption of linear alkane thiols from flat Au is significant also when surfaces are dipped in hexadecane at 83 °C, with faster desorption for shorter chain thiols, while at room temperature immersion in 1 M NaOH or HCl does not affect monolayers of octadecanethiol over 24 h periods.¹⁷ On the other hand, immersion of gold monolayers of alkanethiols, hydroxyalkanethiols and tetraethyleneglycolalkanethiols in serum-free or 10% FBS

(fetal bovine serum) supplemented culture media at 37 °C for short time (30 min) do not evidence desorption.¹⁸ Under similar conditions (TRIS-buffered saline solution at 37 °C for up to 7 days), hydroxoalkanethiol monolayers are also stable.¹⁹ Stepping to thiol coatings on colloidal solutions of GNP, literature evidences that competing thiols can displace grafted thiols on coated spherical GNP even in water and at room temperature,^{20,21} although, depending on the nature of the grafted thiols, poor or nihil displacement may even take place.²² Besides thiol exchange, temperature increase over room temperature has been reported to result into thiol desorption from spherical^{23,24} and rod-like gold nanoparticles.¹⁵

The biocompatible polyethylene glycols (PEGs), equipped with terminal –SH groups, are very frequently used as coatings for GNP, due to their many advantages in bio-medical applications. PEG-coated GNP display improved pharmacokinetic properties,²⁵ PEG enhances *in vitro* stability of GNP in saline buffers or culture media²⁵ and it allows the coated nanoparticles to evade macrophage-mediated uptake and removal from systemic circulation *in vivo*.¹¹ PEG coating is also employed for nanoparticle specific functionalization, as many commercial PEGs in addition to a thiol function suitable for grafting on gold feature also a remote function (*e.g.* -OH, -COOH, -NH₂) that may be used for further chemical modification.^{26,27} Gold nanoparticles modified with fluorescent dyes are also proposed for biomedical applications as image-enhancing agents^{28,29} and as biosensors,^{30,31} with the dyes typically grafted to the gold surface through a remote thiol moiety. It must also be added that GNP have relevant applications in hyperthermal treatments,² as when irradiated on their LSPR they thermally relax, with a highly localized temperature increase. This is particularly interesting when non-spherical nanoparticles are considered, such as gold nanorods (GNR)³² and gold nanostars (GNS).^{33,34} In the latter cases one or two LSPRs are placed in the near-IR range (750-1100 nm) where tissues and blood are semi-transparent, so that non-invasive through tissues localized hyperthermal therapies may be envisaged. Recently, photothermally responsive GNS have been demonstrated to be very efficient *in vitro* against tumours³⁵ and bacterial biofilms.³⁶

In this context the photothermally-triggered release of molecular species adhering to gold nanoparticles may be considered a powerful tool for biomedical applications³⁷ as it might offer a synergistic therapeutic effect through the localized drug release in addition to direct local hyperthermal treatments.

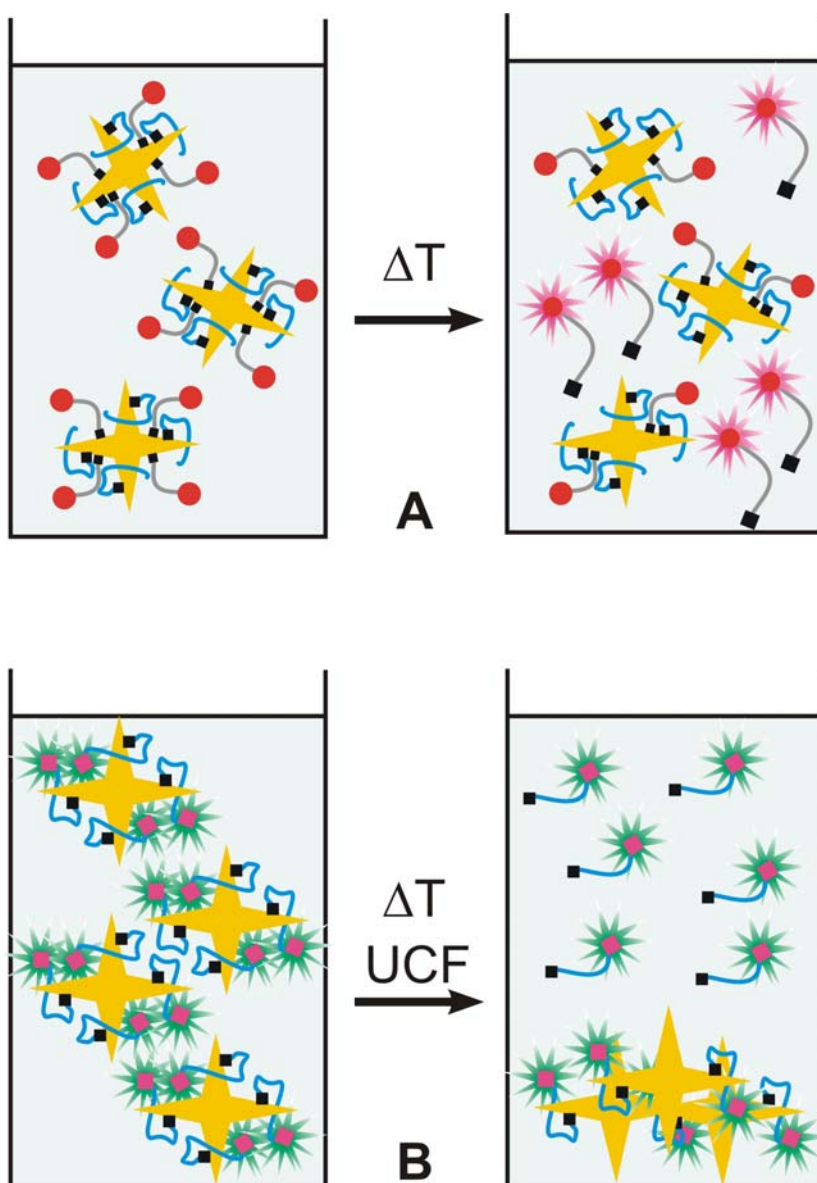


SCHEME 1. Formula of HS-PEG (MW=2000), BDP-SH and HS-PEG-NHTRITC. Picture A is a TEM image of the used GNS, pictures B and C are pictorial sketches of the GNS-PEG-BDP and GNS-PEGNHTRITC constructs

On the other hand the stability of thiol-grafted PEG coatings is typically neglected and taken as assured under all conditions, although under NIR irradiation or even at the temperature typical for in-vivo use (36-42°C) the reviewed literature (refs 15-24) indicates that the S-Au bond is labile and thiols may undergo detachment and displacement by competing species.

Based on this background, the study of the lability of thiolate-grafted coatings of photothermally responsive GNS in aqueous solutions as a function of the temperature and of the nature of

codissolved solutes is particularly relevant. To this purpose we exploited the gold-induced fluorescence quenching of organic dyes that is observed when these are grafted to gold at a short distance.³⁸⁻⁴⁰ The current study was carried out using a model compound, BDP-SH (see **Scheme 1**), containing the Bodipy fluorophore moiety and a remote thiol group, grafted on GNS with PEG-SH as the co-coater, see Scheme 1B. Bodipy dyes are stable in aqueous solutions and have high fluorescence quantum yields⁴¹ with absorption at 500–530 nm,⁴² a range only partially superimposed to the LSPR of GNS.³⁴ In the present paper GNS were obtained by the well-established lauryl sulfobetaine (LSB) assisted synthesis.^{6,34} These GNS are mainly pentatwinned branched nanostars (70-80%), see Scheme 1A, with LSPR tunable in the 750-1100 nm range^{34,36} and centered at ~ 730-750 nm in the synthetic conditions chosen for this paper. Moreover, it was previously demonstrated that they are photothermally active in aqueous solutions, with specific absorption rate (SAR) as high as 80kW/g,³³ and with a local increase in temperature at 10 nm from the gold nanostar surface as high as 12°C.³³ Bodipy fluorescence is strongly quenched by energy transfer to gold nanoparticles,⁴³⁻⁴⁶ while it is revived when Bodipy is detached and released in solution. We used the recovery of the BDP-SH fluorescence signal as an indicator of the fraction of released dye from GNS co-coated with BDP-SH and PEG-SH, as sketched in Scheme 2A. Temperature variations were studied both by heating GNS solutions with a thermostat and by irradiation of GNS on their NIR LSPR. Environmental conditions other than temperature were also investigated, such as biological buffers (PBS and RPMI-1640 cell culture broth) and acidic pH values as those found in endosomes, where nano-objects may experience pH values significantly lower than neutral values.^{47,48} In parallel, the detachment of PEG-SH under the same conditions was also studied, coating GNS with an α -thiol- ω -amino PEG, targeted on the terminal -NH₂ group with the fluorescent tetramethylrhodamine isothiocyanate dye, see Scheme 1C .



SCHEME 2. Pictorial sketch of the approach used to determine the released BDP-SH (A) and HS-PEGNHTRITC (B) from GNS. In case A, BDP-SH fluorescence is quenched when it is grafted to GNS and desorption from GNS due to T increase is measured by fluorescence revival. In case B, the TRITC moiety is fluorescent also when HS-PEGNHTRITC is grafted to GNS. T increase results in HS-PEGNHTRITC desorption from GNS and after separation from GNS by UCF its fluorescence intensity is measured on the supernatant solution.

In this case the fluorescent moiety is too distant from the gold surface to observe emission quenching when grafted to GNS, so we adopted a different approach based on supernatant analysis after separation by ultracentrifugation (UCF) see Scheme 2B. By this we obtained a wide picture on the photothermally induced release of surface-bound thiolated drugs and on the stability of thiol coatings in conditions similar to *in vivo* ones.

2. EXPERIMENTAL

2.1 Chemicals and GNS synthesis. Chemicals were purchased from Sigma-Aldrich or Euroclone Cytogenetics and used as received. Additional details can be found in the *Supporting Information* (S1.1 Chemicals). BDP-SH was synthesized as reported previously.⁴² GNS solutions were obtained by seed growth synthesis with the zwitterionic surfactant LSB as already described.^{6,34} The growth parameters were chosen in order to obtain the LSPR of the prevalent product (pentatwinned branched GNS) in the 730-750 nm range.^{6,34} Full details are described in the SI (S1.2 GNS Synthesis). After the growth process, GNS solutions were ultracentrifuged, the supernatant discarded, the GNS pellet was redissolved in the starting volume of bidistilled water and used for further coating.

2.2 Co-coating of GNS with PEG-SH and BDP-SH. This was carried out by simultaneously adding 100 μ l of 10^{-3} M ethanol solution of BDP-SH and 100 μ l of a 10^{-3} M of aqueous solution of PEG-SH to 10 ml of a GNS solution prepared as described in 2.1 (both thiols are thus 1×10^{-5} M). The obtained solution was allowed to equilibrate for 3 hours at room temperature while gently shaken on a reciprocating shaker. Excess of PEG-SH and BDP-SH was removed by ultracentrifugation (25', 13000 rpm), supernatant discarding, pellet redissolution in 10 mL of bidistilled water. The cycle was repeated two more times to assure complete elimination of unbound PEG-SH and BDP-SH. These were our stock solutions, that were stored in the dark at 4 °C. The stock solutions (bound dye concentration is 5.6 ± 0.5 μ M) were diluted with bidistilled water or other media in 1:10 ratio for further measurements.

2.3 GNS coating with HS-PEG-NH₂ and conjugation with TRITC. This was carried out in two steps. The first was coating with HS-PEG-NH₂. It followed a procedure analogous to that described in the previous section, apart from the addition of the sole bifunctional PEG (200 μ l of a HS-PEG-NH₂ 10^{-3} M aqueous solution). Purification from unreacted HS-PEG-NH₂ was obtained by two ultracentrifugation / redissolution cycles. In the second step, the TRITC dye was conjugated with the grafted bifunctional HS-PEG-NH₂ via reaction of the terminal amino group of PEG with the

isothiocyanate group of TRITC leading to formation of thiourea linkage. 200 μL of 10^{-3} M of TRITC solution (same molar quantity of the HS-PEG-NH₂ added in the previous step) in anhydrous DMF was added to a 10.0 mL solution of GNS coated with SH-PEG-NH₂ and the obtained solution was kept overnight under gentle stirring on a reciprocating shaker at room temperature. Removal of possible unreacted TRITC was obtained by two ultracentrifugation/ redissolution cycles. Further details in the SI (section 2.3).

2.4 Spectroscopy measurements. Absorbance spectra were recorded using a UV/VIS/NIR spectrophotometer V-570 (Jasco). The emission spectra were recorded using an Eclipse spectrofluorimeter (Varian, AU). The detector gain (800 V) and the slits size (exc. slit 5 nm; em. slit 10 nm) were kept constant over all the measurements. BDP-SH was excited at 525 nm and its maximum emission intensity was observed at 539-541 nm. TRITC dye was excited at 555 nm. The maximum emission intensity was observed at 578-580 nm.

2.5 Dynamic light scattering (DLS). DLS was performed using a homemade setup described elsewhere.⁴⁹ DLS measurements were taken on the solutions before and after the temperature treatments. We investigated the average size and the size distribution for $T = 20\text{ }^{\circ}\text{C}$, $42\text{ }^{\circ}\text{C}$ and $50\text{ }^{\circ}\text{C}$ (see SI, S9. *DLS of the decorated GNS solutions*). The size distributions were computed by applying maximum entropy methods^{50,51} to the modulus of the electric field correlation function according to the integral equation described in SI (S9. *DLS of the decorated GNS solutions*).

2.6 Bulk temperature control. For fluorescence studies of BDP-SH and HS-PEGNHTRITC release as a function of the bulk temperature, a 2 mL volume solution of GNS co-coated with BDP-SH and PEG-SH was prepared by diluting 0.2 mL of the stock solution with 1.8 mL of MilliQ water. The temperature control was obtained with a Cary Temperature Controller connected to the Varian spectrofluorimeter.

2.7 Near Infrared Irradiation. The release of BDP-SH from GNS was triggered also by irradiating the nanoparticle suspension at $\lambda = 800\text{ nm}$ (Tsunami, Spectra Physics, CA, pulse repetition rate 80 MHz, pulse width 200 fs). The laser was focused on a small volume (30 μL) at the bottom of an

Eppendorf cuvette of which approximately 22 μL were irradiated with average intensity in the range $0.14 \text{ W/cm}^2 \leq I \leq 2.9 \text{ W/cm}^2$, assuming a beam diameter $\approx 3 \text{ mm}$. The temperature changes were monitored by means of a Thermovision camera (FLIR, USA) with supporting software.

2.8 Quantitative determination of the boron bound on GNS by inductively coupled plasma optical emission spectroscopy (ICP-OES). A 5 mL sample of GNS solution after the described co-coating procedure was diluted to 10 mL, ultracentrifuged (13000 rpm, 20 minutes), the supernatant discarded and GNS pellet on the bottom was redissolved in bidistilled water. The procedure was repeated two more times. After the final ultracentrifugation the supernatant was discarded and the pellet treated with 1.0 ml bidistilled water plus 2.0 ml of freshly prepared aqua regia. The blue color of GNS immediately disappeared and after 24 hours the solution was analyzed with ICP-OES, using an Optima 3300 DW, Perkin Elmer instrument.

3. RESULTS AND DISCUSSION.

3.1 GNS co-coated with BDP-SH/PEG-SH. The GNS used in this paper are prepared according to literature,^{6,34} and are prevalently pentatwinned branched nanoparticles (TEM image in SI, FigureS4) with LSPR maximum at 730-750 nm. Previous characterization studies³⁴ showed that these have average branch length of 30 nm with negative zeta potential, ζ -potential = -15 mV . Coating is carried out on GNS by adding a mixture with 1:1 molar ratio BDP-SH:PEG-SH. Coating makes the LSPR to red-shift of $\sim 30 \text{ nm}$ (SI, Figure S3.1.1), as typical of these GNS^{6,34} when the local refractive index increases due to the surface grafting of molecules less hydrophilic than water, like BDP-SH. The coated GNS (species B in Scheme 1) are stable to repeated ultracentrifugation cycles and are not affected by high NaCl concentration (no spectral changes are observed over 4 hours in 0.01-1 M NaCl⁵²). Their Z potential is -9 mV in pure water and -1 mV in 0.1M NaCl Using a 1:1 molar ratio in the coating process, however, does not mean that the two thiols are equimolar also on the GNS surface. It has been shown that the tendency of two competing thiols to graft on an Au surface from the same solution is inversely proportional to their affinity to the solvent.⁵⁵⁻⁵⁹ In this

case, being BDP-SH poorly soluble and PEG-SH fairly soluble in water, we should expect an higher surface fraction of the former. We have obtained sharp analysis of the coating composition of this GNS type by Differential Scanning Calorimetry (DSC) on dry GNS samples.^{34,53}

Unfortunately in this case GNS co-coated with BDP-SH and PEG-SH are not stable under the drying and heating procedures (spurious peaks are observed when DSC is carried out). However, we are able to calculate both the concentration and the number of BDP-SH molecules per GNS in our stock solutions: from ICP-OES on GNS oxidized with aqua regia we obtain boron and gold concentrations. B, contained in BDP (see Scheme 1) gives directly the BDP-SH concentration, $5.36 \times 10^{-6} \text{M}$. Au is $2.36 \times 10^{-4} \text{M}$. The average number of BDP-SH molecules per single GNS in the samples, ~ 3400 , is obtained using the average GNS mass, that we have calculated in a previous paper ($5 \times 10^{-17} \text{g/GNS}$, see ref 53). The co-coated GNS are resistant to 3 or more ultracentrifugation / redissolution cycles, indicating that a consistent quantity of PEG is grafted on their surface. As a further point to support this we carried out preparations with the same total added thiol (BDP-SH + PEG-SH = $2 \times 10^{-6} \text{M}$) but also with 0.1 to 1.0 BDP-SH:PEG-SH molar fraction in the coating solution. Coated GNS are stable to 3 or more ultracentrifugation cycles only for BDP-SH molar fractions 0.1-0.7. Higher molar fractions in the coating solutions give less stable coated GNS, due to the small quantity of grafted PEG-SH. The number of BDP-SH per GNS varies from 2900 to 3600 along the 0.1-0.7 molar fraction series with a linear increase with the BDP-SH molar fraction in the coating mixture (see SI, Table S2.2.1 and Figure S2.2.1).

GNS are non-spherical and one may hypothesize that they have zones in which the coating is more exposed to water (*e.g.* tips) with respect to other less hydrated zones (*e.g.* cavities between branches). One may thus also wonder if a preferential disposition of PEG-SH (on tips) and BDP-SH (in cavities) holds, with a “isles” morphology of the two coaters instead of a random distribution. Vicinal fluorophores, typical of an isles-like preferential distribution, may give self-quenching, as it is found *e.g.* on spherical GNP.⁵⁴ It should be expected that the effect is more intense with increasing surface concentration of BDP-SH. However we examined the fluorescence intensity of

the series of GNS with different BDP-SH molar fractions in the coating solution, and found a linear increase with the latter, with no changes in the shape of the emission spectra (SI, Figures S3.2.1 and S3.2.2)

Finally, the concentration of BDP-SH bound to the coated GNS used in this work (*i.e.* prepared with 1:1 BDP-SH/PEG-SH and used as stock solutions) was calculated also optically. This was done by absorption spectrophotometry, using the BDP-SH extinction coefficient at 525 nm calculated in ethanol ($\epsilon_{525} = 4.48 \pm 0.2 \cdot 10^4 \text{ M}^{-1} \text{ cm}^{-1}$) and correcting the absorbance at 525 nm of the coated GNS by subtracting the contribution of the uncoated GNS (details in the SI, section 3.1). The obtained value is $5.6 \pm 0.5 \times 10^{-6} \text{ M}$, in full agreement with the ICP-OES data. This is the concentration of the stock solution used in this paper.

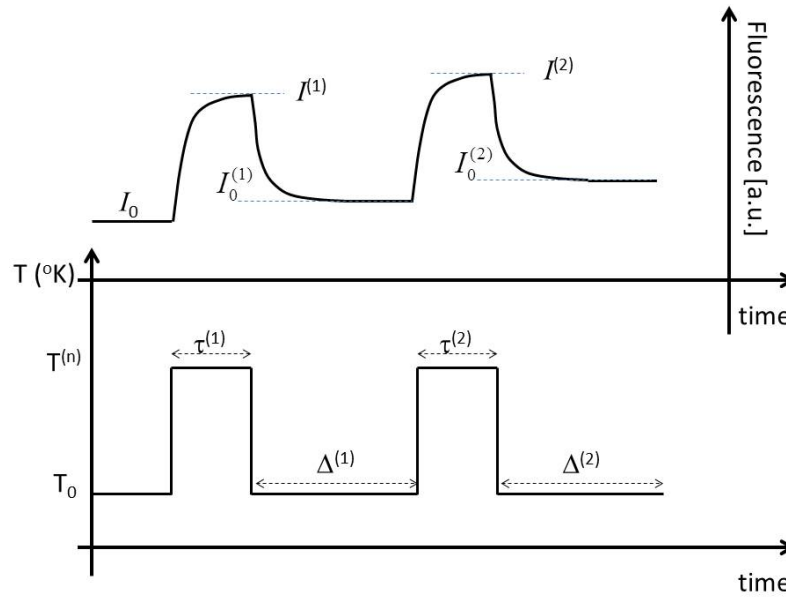
3.2 Estimate of released BDP-SH as a function of bulk temperature. The fluorescence yield (ratio of the fluorescence emission to the dye concentration) of the grafted BDP-SH as a function of the temperature cannot be measured directly, since the dye is released from the GNS surface as the temperature increases. . Moreover, the fluorescence yield of free BDP-SH decreases with increasing temperature (see SI, section S6). Therefore a temperature cycling procedure has been adopted in order to follow the dye release through the changes of its fluorescence signal, thus circumventing the variations due to the fluorescence yield variation with T. The temperature cycle, shown in Scheme 3, started from the solution at temperature $T_0 = 20 \text{ }^\circ\text{C}$ whose fluorescence is I_0 , then a rapid ($<30 \text{ sec}$) increase of the suspension temperature to $T^{(n)} > T_0$ was obtained where the fluorescence intensity $I^{(n)}(t)$ was measured for a time stretch $\tau^{(n)}$. The temperature was then rapidly ($<30 \text{ sec}$) decreased back to T_0 , where the fluorescence $I_0^{(n)}(t)$ was followed in time for a time stretch, $\Delta^{(n)}$. The cycles where repeated N times ($n=1,2,\dots,N$). In this protocol we assumed that all BDP-SH was bound to GNS before starting the temperature treatment, this allowing to calculate the fluorescence yield for the bound fluorophore at $20 \text{ }^\circ\text{C}$, $\eta_B(20) = 71.2 \pm 6 \text{ (a.u.)}$. We also assumed that the kinetics of dye re-grafting to GNS occurred on a scale much longer than the cooling time ($< 30 \text{ sec}$): the last

assumption was verified experimentally *a posteriori*. The fluorescence yield of the free fluorophore at 20 °C can be measured on pure BDP-SH, $\eta_f(20) = 2180.8 \pm 4$ (a.u.)

We use a simple relation between the fluorescence emission of samples measured at $T=T_0$ (independent of the heating history of the sample) and the concentration of the BDP-SH released in the suspension ($C_f^{(n)}$):

$$\begin{cases} I_0^{(n)} = \eta_f(20)C_f^{(n)} + \eta_b(20)C_b^{(n)} = \\ \quad = [\eta_f(20) - \eta_b(20)]C_f^{(n)} + \eta_b(20)C_{tot} \\ \quad = \Delta\eta_{fb}C_f^{(n)} + I_0 \end{cases} \quad (1)$$

with $C_b^{(n)}$ = concentration of the bound BDP-SH and $C_{tot} = C_b^{(n)} + C_f^{(n)}$. C_{tot} is the the concentration of the stock solution diluted 1:10 for the fluorescence experiments, i.e. 0.56×10^{-6} M.



Scheme 3. Sketch of the typical bulk temperature cyclic experiment on the Bodipy decorated GNS solutions. The lower panel reports the temperature kinetics. The transitions between the lower (T_0) and the upper ($T^{(n)}$) temperatures are much shorter than the typical incubation time and are sketched

as abrupt changes. The upper panel reports a sketch of the fluorescence emission kinetics both in heating up and in re-cooling.

An explicit expression for the concentration of the released dye is then obtained as:

$$C_f^{(n)} = \frac{I_0^{(n)} - C_{tot}\eta_b(20)}{\Delta\eta_{fb}} = \frac{[I_0^{(n)} - I_0]}{\Delta\eta_{fb}} \quad (2)$$

leading to an expression for the fraction of released dye p_{BD} as:

$$p_{BD}^{(n)} = C_f^{(n)} / (C_{tot}) \quad (3)$$

The above algorithm does not imply any assumption on the temperature dependence of the fluorescence yield of the bound species.

3.3 Thermal stability of the thiol bonding in aqueous media: single temperature jump. The fraction of released BDP-SH from the coated GNS due to a single exposure at $T^{(1)} > T_0 = 20^\circ\text{C}$ for a time lapse in the range $10 \text{ min} \leq \tau^{(1)} \leq 40 \text{ min}$ (see **Scheme 3**), $p_{BD}^{(1)}$, was investigated by monitoring the BDP-SH emission and the results are shown in **Figure 1A**. We always found that after bringing the suspension temperature back to $T_0 = 20^\circ\text{C}$ the BDP-SH fluorescence was higher than the pre-heating value, $I_0^{(1)} > I_0$.

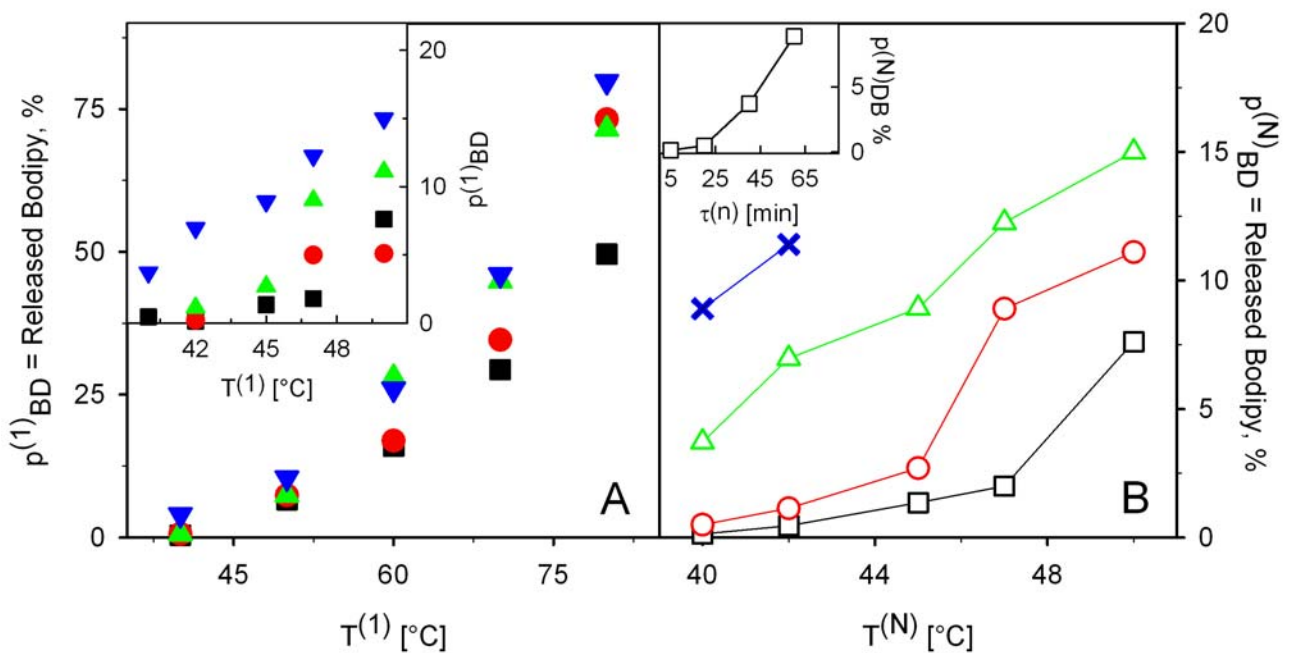


Figure 1. Temperature treatments of GNS-PEG-BDP in water solutions. **Panel A:** Single cycle experiments reporting the % fraction of released BDP-SH from coated GNS as a function of temperature. The symbols refer to incubation times $\tau^{(1)} = \Delta^{(1)} = 5$ min (full black squares), 10 min (full red circles), 20 min (full green up triangles) and 40 min (full blue down triangles). The inset shows a blow up of the region $37\text{ °C} \leq T^{(1)} \leq 50\text{ °C}$. **Panel B** (lines are added to guide the eye): Repeated (N=3) temperature cycling experiments showing the influence of temperature ($T^{(N)}$ is the higher temperature of the cycle) and incubation time, $\tau^{(n)}$, on BDP-SH release for $\tau^{(n)} = 5$ min (empty black squares), 20 min (empty red circles), 40 min (empty green triangles) and 60 min (empty blue stars). $\Delta^{(n)} = \tau^{(n)}$. The inset reports the released dye fraction (N=3, $T^{(N)} = 40\text{ °C}$) as a function of $\tau^{(n)}$. Uncertainties on the data are between $\pm 0.25\%$ and $\pm 0.35\%$.

This suggests that a fraction of BDP-SH was released at high temperature and was not resorbed on the GNS surface when the suspension was rapidly (within 30 sec) brought back at $T=T_0$. By applying Equations (2,3), we obtain a fraction of released dye $p_{BD}^{(1)} > 3\%$ only for temperatures above 45 °C , which is however outside the physiological range $37\text{--}42\text{ °C}$. To be noted that a value of 3% is ~ 8 times our experimental uncertainty (Figure 1A).

For values of $T^{(1)}$ close to the room temperature and in any case for $T^{(1)} \leq 37\text{ °C}$, the thiol bonding *in aqueous solutions* appears quite stable even for prolonged exposures ($p_{BD}^{(1)} \leq 4\%$ for $T^{(1)} < 40\text{ °C}$ and $\tau^{(1)} \leq 40'$, Figure 1A).

3.4 Thermal stability of the thiol bonding under temperature cycling. As shown in section 3.3, below $T^{(1)} = 50\text{ °C}$ the effect of the incubation time on $p_{BD}^{(1)}$ appears only for long heating times. Nevertheless, understanding the release trend at temperatures below 50 °C is essential for biomedical application, in which prolonged and repeated photothermal treatments could be carried out with the same GNS batch. Accordingly, we tried to increase the released dye fraction in the range $40\text{ °C} \leq T^{(n)} \leq 50\text{ °C}$ by performing repeated (N=3) cycles ($20\text{ °C} \rightarrow T^{(n)} \rightarrow 20\text{ °C}$)_{n=1,...,N} with

different incubation times $\tau^{(n)}$ and $\Delta^{(n)} = \tau^{(n)}$ (Figure 1B). The fraction of released dye was computed according to (3) from the fluorescence intensity, $I_0^{(N)}$ (see Scheme 3), measured after the suspension was recooled to room temperature, T_0 , after the last heating cycle.

As it can be seen from Figure 1B, incubation times from $\tau^n = 5$ min to $\tau^n = 20$ min did not significantly impact on the release of BDP-SH in the range 40-45°C ($p_{BD} < 2.5\%$). However, For $\tau^n = 40$ min or above, the fraction of released dye rose to 9 – 11 % at $T^{(3)} = 40$ °C – 42 °C (Figure 1B, stars). The released dye fraction increased non linearly with the incubation time (Figure 1B inset). Moreover, it was found that the reduction of the relaxation time at 20°C to $\Delta^{(n)} \sim 4-5$ min $\leq \tau^{(n)}$ while performing these cycles led to an increase in the fractions of released BDP-SH. At $T^{(n)} = 40$ °C the BDP-SH released fraction of $\sim 10\%$ ($\Delta^{(n)} = 5$ min, $\tau^{(n)} = 40$ min) was reached and this value raised to $\sim 15\%$ for cycling at $T^{(n)} = 50$ °C.

3.5 Full BDP-SH release from GNS at $T^{(n)} = 80$ °C. In the previous analysis we relied on the assumption that BDP-SH was initially completely bound to gold nanostars in our GNS-PEG-BDP solutions. The degree of approximation of this assumption was verified by performing repeated ($N = 15$) cycles $T^0 \rightarrow T^{(n)} \rightarrow T^0$ at a very high temperature, $T^{(n)} \sim 80$ °C, for intermediate values of incubation times $\tau^{(n)} = 10$ min and $\Delta^{(n)} = 10$ min. We reasoned that in this way we should be able to completely release the BDP-SH bound to the gold nanostars. The concentration of the dye obtained by equation (3) was compared with the values obtained from the absorption spectrum of the GNS-PEG-BDP construct under the assumption that the dye extinction coefficient was not significantly affected by the vicinity of the gold nanoparticles surface. The values of intensity, $I_0^{(n)}$, measured at the end of each of the $\Delta^{(n)} = 10$ min incubation periods at $T = 20$ °C are reported in Figure 2 (blue squares) and display an overall exponential growth that can be fitted according to

$$I_0^{(n)}(t) = I_\infty - \Delta I e^{-\frac{t}{t_{rel}}}. \text{ From a single exponential fit (solid line) we obtain } t_{rel} \sim 60 \text{ min for } T=T_0)$$

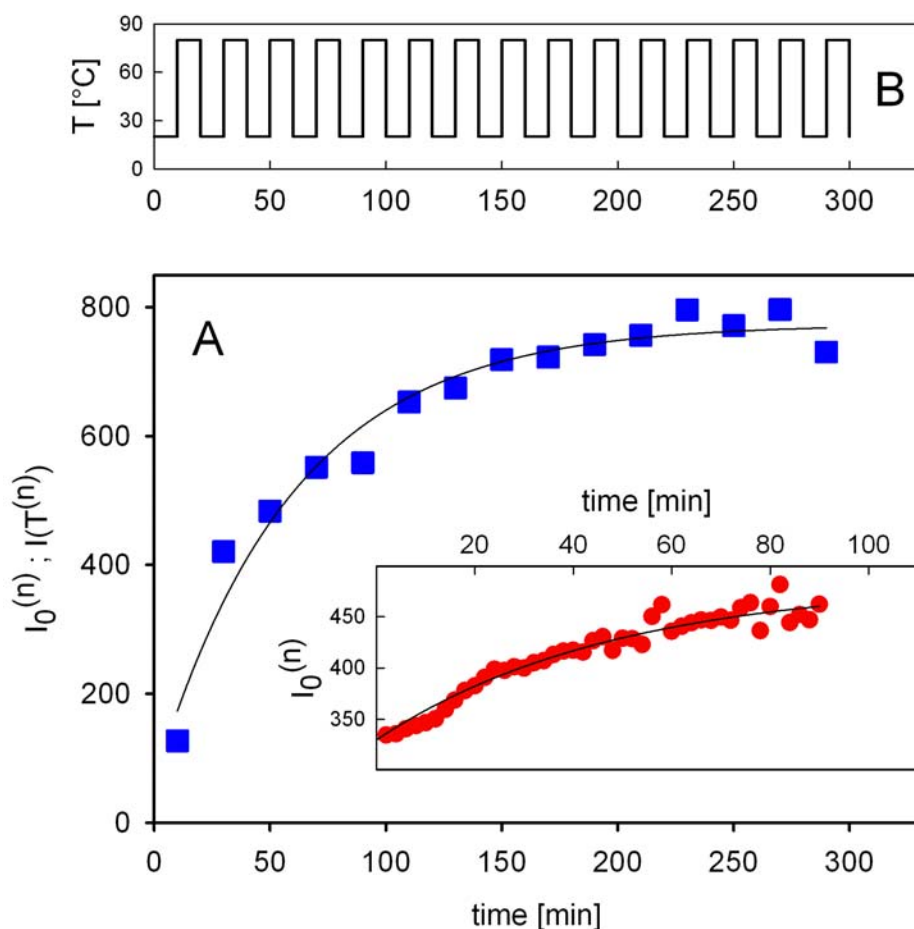


Figure 2. Kinetics of the Bodipy fluorescence emission in water under repeated heating cycles with $n = 1, 2 \dots 15$ and $T^{(n)} = 80$ °C. Panel A: Bodipy fluorescence at the end of each incubation period at $T_0 = 20$ °C ($I_0^{(n)}$, blue squares). The solid line is the best fit to a single exponential growth function. Inset: fluorescence kinetics after bringing the GNS-PEG-BDP suspension at $T^{(1)} = 80$ °C (red circles, single cycle experiment, $\tau^{(1)} = 90$ min). The solid lines are the best fit single exponential growth function to the data. Panel B reports the diagram of the temperature in the solution.

We also followed the change in Bodipy emission during a single long lasting incubation at high temperature $T^{(1)} = 80$ °C. The fluorescence intensity increase could be analyzed as a single exponential growth with relaxation time $t_{\text{rel}} = 48 \pm 4$ min (Figure 2A, inset) smaller than that

measured under alternated heating $t_{\text{rel}} \sim 60$ min ($T=T_0$) (Figure 2A, circles). This result can be explained as a partial resorption of the dye to the gold surface in each low temperature interval. The fraction of dye released in the solution, $p_{BD}^{(n)}$, obtained from the data reported in Figure 2 approached closely 100% ($99\% \pm 0.2$, for $\tau^{(n)} = 10$ min, $N=15$), and the value was independent of the incubation time $\tau^{(n)}$ from 10 min to 60 min (97 ± 0.5 %, for $\tau^{(n)} = 60$ ’, $N=1$). These results confirm the validity of the assumption for the derivation of Equation 1 stating that all (99%) the dye was bound to the GNS surface before starting the thermal treatment and provide the value of bound BDP-SH concentration = 5.6 ± 0.5 μM in stock solutions.

3.6 PEG-SH release induced by temperature. Although the structure, bulkiness and hydrophilicity of the appended groups are very different, PEG-SH and BDP-SH terminate both with a $-\text{CH}_2-\text{CH}_2-\text{SH}$ moiety, see Scheme 1. Accordingly, the nature and the energy of the S-Au bond is expected to be similar between, and a fraction of the grafted PEG-SH could may be as well desorbed on increasing temperature. Being PEG-SH colorless and non-fluorescent, the release of the PEG thiol was studied with a different approach, illustrated by Scheme 2B. A bifunctional HS-PEG-NH₂ was used, and its free primary amino groups were labeled with the TRITC dye (see species C, Scheme 1), thanks to the isothiocyanate-amine coupling reaction, that leads to the formation of the thiourea linkage shown in Scheme 1. TRITC conjugation was carried out with an excess TRITC with respect to the HS-PEG-NH₂ grafted on the GNS, and this is expected to yield the all-functionalized GNS-PEGNHTRITC constructs pictorially described by structure C in Scheme 2. TRITC fluorescence has a maximum of emission (λ_{em}) at 580 nm. Due to the long PEG spacer TRITC dye is not kept near to the gold surface as the Bodipy moiety in BDP-SH and therefore the fluorescence emission of TRITC is not quenched (cartoon on the left of Scheme 2B). The release of TRITC labeled PEG chains was then studied by temperature cycles followed by UCF to separate the released labelled PEG from the GNS suspension (remaining in the supernatant, cartoon on the right of Scheme 2B). The concentration of starting and released PEG is then

determined by fluorimetry. Details on this procedure are described in the SI (Section S10). The results of this analysis show that, during the thermal treatment of the GNS solutions, a PEG-SH chain is also released from the surface of GNS. The fraction of released PEG was $\sim 16\%$ at $T^{(1)} = 37$ °C and raised to $\sim 20\%$ for $T^{(1)} = 42$ °C for incubation time $\tau^{(1)} = 60$ min. Similarly to the experiments aimed at the BDP-SH release, repeated ($N=3$) thermal treatments at high temperature $T^{(n)} = 80$ °C, $\tau^{(n)} = 60$ ’, led to the full release of PEG from the GNS. We must stress that for this analysis GNS were fully coated with a single bifunctional, labelled PEG, a condition different from the GNS-PEG-BDP constructs prepared with a BDP-SH:PEG-SH 1:1 mixed coating solution. Also (see Scheme 1), it may be argued that the bifunctional PEG used in this section has a longer chain than the PEG-SH used for co-coating with BDP-SH. However, focusing on the gold-PEG interaction, the two PEG-thiols are identical up to a distance of 44 ($\text{CH}_2\text{-CH}_2\text{-O-}$) units from the Au surface. It can thus be considered as a reliable data that the fraction of released PEG found here is larger than that of BDP-SH. Moreover this is not surprising, as it is in agreement with the common observation that the competitive deposition of two different thiols, $\text{R}'\text{-SH}$ and $\text{R}''\text{-SH}$, on gold surfaces depends mainly on the differences in the solvent affinity (solubility) of the R' and R'' moieties.⁵⁵⁻⁵⁷ The lower fraction on the surface is found for the most soluble species in the chosen solvent. In the case of GNS-PEG-BDP we deal with the reverse process – release of $\text{R}'\text{-SH}$ and $\text{R}''\text{-SH}$ from a mixed surface – but we may reasonably expect that the thiol with the highest affinity towards water is more easily released. While BDP-SH is poorly water soluble, any PEG polymer is highly soluble in aqueous solutions.

3.7 Temperature induced aggregation. As the previous sections show that a small but significant fraction of both BDP-SH and PEG-SH are released even with small temperature increase, we investigated the effect of temperature also on the aggregation of GNS. This was studied by DLS. The initial (at $T = T_0 = 20$ °C) distribution of the GNS size depends on the typical features of the synthesis (see *SI* for details, section S9). We always found a major, narrow, component (at least 75% in amplitude) with $d_H = 110 \pm 28$ nm (**Figure S9.1**, solid line). This average value was

computed as the z-average over the major component of the distribution $d_H=2R_H$ as described in the *SI* (S9. DLS of the coated GNS solutions). During the temperature cycles ($T^{(n)}=42\text{ }^{\circ}\text{C}$) the size distribution shifts to larger sizes and widens (see **Figure S9.1** and **Figure S9.2A**). It must be noticed that eventually, after $N=3-5$ cycles, we recover at $T=T_0$ a single dominant component of intermediate size $30 \leq d_H \leq 200\text{ nm}$ with at most some tiny contributions for $d_H > 1\text{ }\mu\text{m}$ (see also **Table S9.1**). In all cases the fraction of non-aggregated GNS (*SI* and **Figure S9.1**, inset) is $75\% \pm 15\%$ for $\Delta^{(n)}=5\text{ min}$ and lowers to small values ($\sim 10\%$) only when the incubation time is longer than $\tau^{(n)}=40\text{ min}$. The BDP-SH and PEG-SH release from the Au surface could be responsible of this minor nanoparticle aggregation after temperature treatments. This may also affect the kinetics of resorption of the dye to the gold surface.

3.8 Effect of medium chemical composition and pH on BDP-SH release. For biomedical or biotechnological application coated gold nanostars are diluted in biological fluids, containing salts and proteins that may have effects on the stability of the thiol bonding. To investigate the role of the medium composition, single temperature jumps and temperature cycles were carried out on GNS co-coated with 1:1 PEG-SH and BDP-SH, dissolved in Phosphate Buffered Saline (PBS, stock and 1% solutions), RPMI media, and in acidic buffer. The used $T^{(n)}$, $\Delta^{(n)}$ and $\tau^{(n)}$ parameters were as described in pure water (sections 3.3 and 3.4). Although in-vivo the formation of “corona” due the nanoparticles interaction with a range of biomolecules should be taken into account, the biological fluids investigated here cover at least a wide range of properties. PBS, a buffer frequently used in biological applications especially for preliminary researches *in vitro*, is an aqueous saline solution at pH 7.4 based on sodium and potassium chloride and hydrogen phosphate (chloride concentration ca 0.15 M) without magnesium or calcium. RPMI-1640 cell media is widely applied for supporting the growth of many types of cultured cells, and it contains amino acids and high concentrations of vitamins and salts. The fraction of BDP-SH released in these media was computed from the fluorescence emission of the solutions after they were recooled at $T_0 = 20\text{ }^{\circ}\text{C}$ according to equations (2)–(4). A significantly larger temperature-induced dye release was measured in PBS solutions

(green circles, Figure 3A) with respect to what was observed in pure aqueous solutions (blue triangles, Figure 3A). Repeated temperature cycles ($N=3$, $\tau^{(n)} = 40$ min; $\Delta^{(n)} = 5$ min) were then performed for $T^{(n)} = 30, 34, 37, 40$ and 42 °C in PBS and RPMI media and compared with pure water. The results, shown in Figure 3B, indicated that the largest dye release was obtained in RPMI ($\sim 40\%$ dye release at $T^{(n)}=40$ °C), although also PBS media enhances BDP-SH release ($\sim 20\%$ dye release at $T^{(n)}=40$ °C), compared to the poor release of BDP-SH in pure aqueous medium.

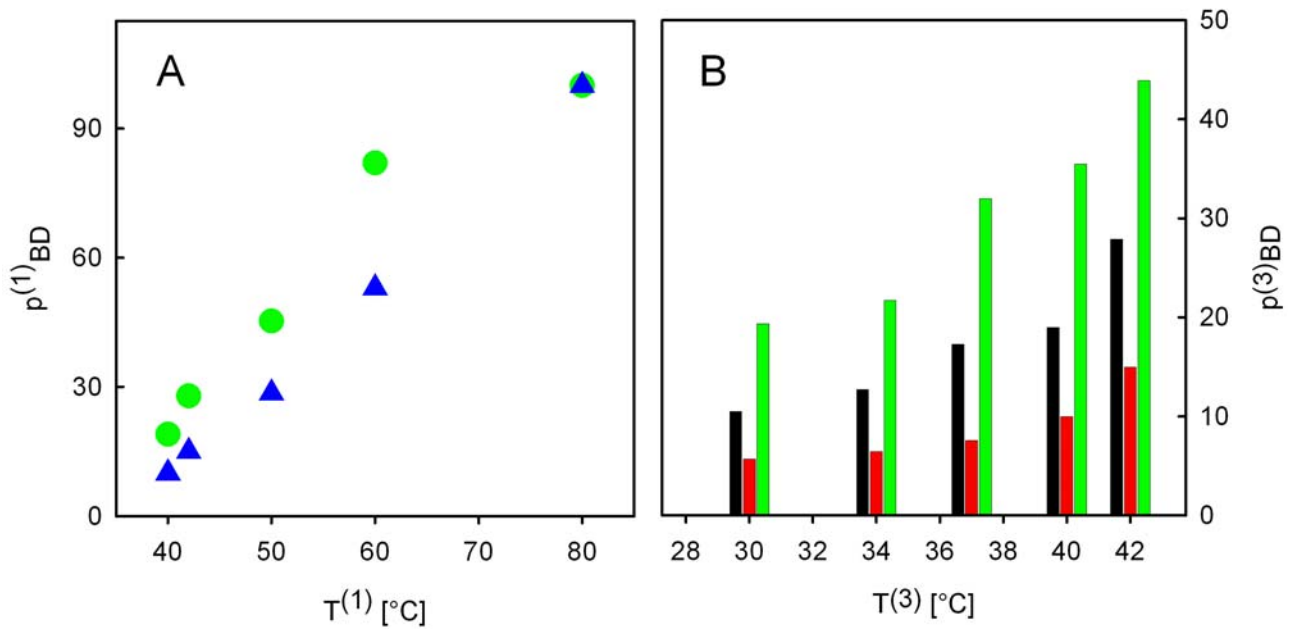


Figure 3. A: Release of Bodipy in aqueous (blue triangles) and in PBS solutions (green circles) in the range $40 \leq T^{(n)} \leq 80$ °C for a single step cycle. B: fraction of released dye measured for a three steps cycle ($N=3$) in the temperature range 30-42 °C for aqueous (red bars), PBS stock (black bars) and for RPMI (green bars).

The media composition affects also the kinetics of the desorption and resorption of BDP-SH from GNS, which is a valuable information for pharmacological treatments. After a complete dye release reached by exposing the GNS solutions at $T^{(1)} = 80$ °C ($N=1$), we monitored by means of fluorescence decay the spontaneous resorption of the dye occurring when re-cooling the suspension to $T_0 = 20$ °C. The measured kinetics can be described by a single exponential component =

$\exp[-t/\tau_{\text{rel}}]$ (see *SI: S7. Kinetics of dye resorption after full release*, **Figure S7.1**) with very long relaxation times., For the aqueous and PBS solutions $t_{\text{rel}} \sim 120$ hours.

Finally, since the intracellular environment is mainly acidic,⁴⁷ we also monitored the BDP-SH emission intensity in acidic media during temperature treatments. Mild cycles ($T_0 = 20$ °C; $T^{(n)} = 42$ °C; $\tau^{(n)} = 40$ min, $N=3$) were performed in acidic buffer at pH 4.2 and we measured BDP-SH release up to 40% (**Table S6.6**). Moreover, after the release of the dye in acidic media the emission intensity of dye decreased dramatically due to degradation of the Bodipy moiety in these media.⁵⁸ This fact was additionally verified by performing the same cycles with solutions of free BDP-SH (see **Tables S6**). For times longer than 40' no substantial increase in the BDP-SH release could be detected (see **Table S6.6**).

3.9 Near infrared irradiation of GNS- PEG-BDP constructs. We have studied the release of BDP-SH from the GNS-PEG-BDP constructs induced by the irradiation of the solutions with NIR laser radiation tuned at $\lambda = 800$ nm, *i.e.* within the LSPR of these GNS (**Figure S3.1.1**). We assumed that the release was an indirect effect of the LSPR absorption by the GNS, that thermally relax resulting in a T increase of the solution.^{34,59} First, we have investigated the effect of the laser intensity and of the nanoparticle concentration on the suspension temperature, using 20-fold concentrated GNS solutions with respect to stock solutions. This was found to increase versus time with a double exponential trend up to a plateau value (**Figure 4**). The slower relaxation component can be ascribed to the exchange of the solution with the laboratory environment, of the order of 150-500 s (see *Supporting Information*) and accounts for at least half of the overall temperature increase (see **Figure 4** and *SI*, **Figure S12.1**). The faster component can be ascribed to the heat exchange within the irradiated suspension.⁵⁹ The overall increase of the suspension temperature has a linear dependence on the irradiation intensity $\langle I \rangle$. However we observed a reduced dependence of the temperature increase on the GNS concentration (**Figure 4B**): the slope $\partial \Delta T / \partial \langle I \rangle$ changes from 5 ± 0.2 [°C·cm²/W] for $C = 0.39$ mg/mL to 15 ± 2 [°C·cm²/W] for $C = 0.78$ mg/mL and does not substantially increase raising the concentration to $C = 1.95$ mg/mL ($\partial \Delta T / \partial \langle I \rangle = 17 \pm 0.2$

[°C·cm²/W]). This is likely due to the overall extinction (scattering and absorption) of the NIR radiation by the nanoparticles with a reduction of the effective radiation that can be absorbed by the GNS.

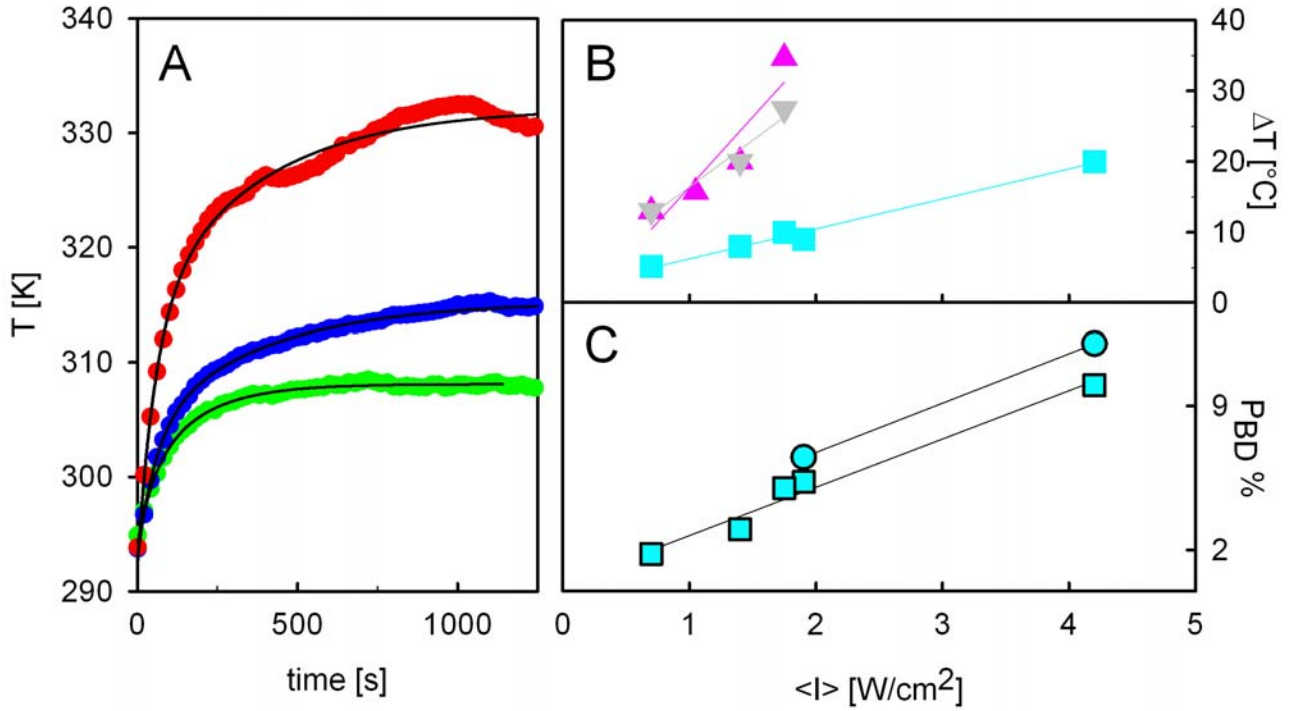


Figure 4. Panel A: NIR induced temperature increase in GNS-PEG-BDP solutions. Symbols refer to NIR intensities $\langle I \rangle = 0.7$ (green circles), 1.4 (blue circles) and 1.8 (red circles) W/cm². Solid lines are data best fits to the function $T_{\infty} - \Delta T_{fast} \exp(-t/\tau_{fast}) - \Delta T_{slow} \exp(-t/\tau_{slow})$. The GNS concentration was $C = 0.78$ mg/mL. **Panel B:** solution temperature increase for $C = 0.39$ mg/mL (cyan squares), 0.78 mg/mL (grey down triangles), 1.95 mg/mL (purple up triangles). Lines are linear best fits with slopes: 17 ± 2 [°C·cm²/W] ($C=1.95$ mg/mL), 15 ± 2 [°C·cm²/W] ($C=0.78$ mg/mL) and 5 ± 0.2 [°C·cm²/W] ($C=0.39$ mg/mL). **Panel C:** fraction of released Bodipy as a function of $\langle I \rangle$ for treatment duration $\tau^{(1)} = 40'$ (cyan squares) and $\tau^{(1)} = 60'$ (cyan circles; $C=0.39$ mg/mL). The lines are linear best fits with slopes: 2.4 ± 0.1 [cm²/W] ($\tau^{(1)} = 40'$) and 2.9 ± 0.2 [cm²/W] ($\tau^{(1)} = 60'$).

Due to the high concentration of GNS in the concentrated samples it was also impossible to collect the fluorescence emitted by the released dye. Therefore the sample was centrifuged (10 min, 13000 rpm) immediately after the NIR irradiation and the emission and excitation spectra of the supernatant were recorded. As a control we measured the emission of the supernatant of a non-irradiated GNS-PEG-BDP solution, finding negligible dye emission ($\lambda_{em} = 540\text{nm}$). Since the concentration of dye in these samples was too low to allow an accurate measurement of the supernatant absorbance, we have exploited the much more sensitive fluorescence signal. In order to quantify the released BDP-SH concentration we calibrated the emission and excitation spectra intensity as a function of free BDP-SH concentration as described in the SI (Section S11). The percentage of the released BDP-SH obtained in this way is summarized in **Figure 4C**. The released fraction increases linearly with the irradiation $\langle I \rangle$ (**Figure 4C**) and correlates with irradiation time (**Figure 4C**). This finding proves the origin of NIR activated release. The amount of released dye is less than 13% even at $\langle I \rangle = 4.2 \text{ [W/cm}^2\text{]}$ and with long irradiation times (60 min). The 20% increase of the slope, $\partial P_{BD}^{\%} / \partial \langle I \rangle$ from $2.4 \pm 0.1 \text{ [cm}^2\text{/W]}$ for irradiation time $\tau^{(1)} = 40 \text{ min}$ to $2.9 \pm 0.2 \text{ [cm}^2\text{/W]}$ for $\tau^{(1)} = 60 \text{ min}$ observed in **Figure 4C**, does not reflect the 50% increase of the irradiation times due to the saturation time of the temperature increase which is of the order of 5-10 min (see **Figure 4A** and **Table S12.1**).

CONCLUSIONS

In this work the stability of thiol bonding on the surface of gold nanoparticles in aqueous solutions and biologically relevant conditions was studied as a function of temperature and solution composition. We used GNS co-coated with the fluorescent dye BDP-SH and PEG-SH, a construct that is representative of nanotools that could be used simultaneously for photothermal treatments and drug delivery. It must be stressed that most of the literature regards the use of thiol-coated spherical GNP and we have used here star-shaped GNP, so some caution should be used on generalizing these results. We have evidenced that a clear effect holds with temperature, decreasing the stability of the thiol bonding even in the narrow physiological range $37^{\circ}\text{C} - 42^{\circ}\text{C}$. Investigation

of the kinetics of desorption and resorption of the BDP-SH to the GNS surface also evidenced that repeated cycling between two temperatures leads to a larger release of the dye from the GNS surface with respect to a single, prolonged, thermal treatment. Moreover, we have evidenced that between the poorly hydrophilic BDP-SH and the strongly hydrophilic PEG-SH, the latter is released in a larger fraction from the GNS surface, consistently with its higher affinity for the solvent. It is even more relevant that the salt, amino acids and vitamins content of the suspending solution has an important detrimental effect on the thiol bonding stability, larger than the pure thermal effect. All these results indicate that the bond between the gold surface and commercial PEG polymers bearing a single -SH function may be not as inert as it is commonly considered, suggesting the need of a careful control of the stability of thiol protective coatings in biological environments, especially when they are to be used in-vivo for prolonged times and for photothermal applications. Copolymers bearing PEG chains and featuring multiple thiol or disulphide functions may be the obvious answer to these drawbacks,⁶⁰ as they offer all the useful properties of PEG and the enormously increased grafting stability due to surface-polymer multipoint interactions. On the other hand, especially in the case of hydrophylic drugs bound with a single thiol to GNP, our work indicates that a photothermally induced local increase of temperature may be an efficient tool to obtain switchable drug release.

ASSOCIATED CONTENT

Supporting Information. The supporting information includes additional data about kinetics of Bodipy and PEG release from GNS under bulk temperature increase, impact of temperatures and media on the intensity of solutions free and bound dye, long term kinetics of dye re-sorption after full release in aqueous media and PBS solutions, temperature activated full release of Bodipy from GNS, DLS measurements, calibration plots of the emission and excitation spectra as a function of free Bodipy concentration, experimental details. This material is available free of charge via the Internet at <http://pubs.acs.org>

AUTHOR INFORMATION

Corresponding Authors

* mykola.borzenkov@unimib.it; * piersandro.pallavicini@unipv.it

Author Contributions

The manuscript was written through contributions of all authors. All authors have given approval to the final version of the manuscript.

ACKNOWLEDGMENT

The authors acknowledge the funding of Fondazione Cariplo, grant № 2010-0454 and MIUR (PRIN 2010-2011, 20109P1MH2_003). The authors are grateful to Sara Perotto for assistance in NIR irradiation experiments.

REFERENCES

- (1) Sperling, R. A.; Pilar, R.; Zhang, F.; Zanella, M.; Parak, W. J. Biological application of gold nanoparticles. *Chem. Soc. Rev.* **2008**, *37*, 1896-1908.
- (2) Huang, X. H.; Jain, P. K.; El-Sayed, I. H.; El-Sayed, M. A. Plasmonic photothermal therapy (PPTT) using gold nanoparticles. *Lasers Med. Sci.* **2008**, *23*, 217-228.
- (3) Anwar, M. K.; Jarrar, B. M. Histological alterations in the liver of rats induced by different gold nanoparticles sizes, doses and exposure durations. *J. Nanobiotechnol.* **2012**, *10*, 5-13.
- (4) Daniel, M.; Astruc, D. Gold nanoparticles: assembly, supramolecular chemistry, quantum-size-related properties, and applications toward biology, catalysis, and nanotechnology. *Chem. Rev.* **2004**, *104*, 293–346.
- (5) Anker, N. J.; Hall, P. W.; Lyandres, O.; Shah, N. C.; Zhao, J.; Van Duyne, R. P. Biosensing with plasmonic nanosensors. *Nat. Mater.* **2008**, *7*, 442-453.

- (6) Pallavicini, P.; Chirico, G.; Collini, M.; Dacarro, G.; Dona, A.; D'Alfonso, L.; Falqui, A.; Diaz-Fernandez, Y.; Freddi, S.; Garofalo, B.; Genovese, A.; Sironi, L.; Taglietti, A. Synthesis of branched Au nanoparticles with tunable near-infrared LSPR using a zwitterionic surfactant. *Chem. Commun.* **2011**, *47*, 1315-1317.
- (7) Huang, H. S.; Hainfeld, J. F. Intravenous magnetic nanoparticles cancer hyperthermia. *Int. J. Nanomed.* **2013**, *8*, 2521-2532.
- (8) Sperling, R. A.; Parak, W. J. Surface modification, functionalization and bioconjugation of colloidal inorganic nanoparticles. *Philos. Trans. R. Soc., A* **2010**, *368*, 1333-1383.
- (9) Zeng, S.; Young, K.; Roy, I.; Dinh, X.-Q.; Yu, X.; Luang, F. A review on functionalized gold nanoparticles for biosensing applications. *Plasmonics* **2011**, *6*, 491-506.
- (10) Han, G.; Ghosh, P.; Rotello, V. M. Multi-functional gold nanoparticles for drug delivery. In *Bio-Applications of nanoparticles*; Warren, C. W., Ed.; Springer Science: New York, 2007; pp 48-56.
- (11) Sanna, V.; Pala, N.; Sechi, M. Targeted therapy using nanotechnology: focus on cancer. *Int. J. Nanomed.* **2014**, *9*, 467-483.
- (12) Dykman, L. A.; Khlebstov, N. G. Gold nanoparticles in biology and medicine: recent advances and prospects. *Acta Naturae* **2011**, *3*, 32-55.
- (13) Gronbeck, H.; Curioni, A.; Andreoni, W. Thiols and disulfides on Au (III) surface: the headgroup-gold interaction. *J. Am. Chem. Soc.* **2000**, *12*, 2839-3842.
- (14) Nuzzo, R. G.; Dubois, L. H.; Allara, D. L. Fundamental studies of microscopic wetting on organic surfaces. 1. Formation and structural characterization of a self-consistent series of polyfunctional organic monolayers. *J. Am. Chem. Soc.* **1990**, *112*, 558-569.
- (15) Gustafson, T. P.; Cao, Q.; Wang, S. T.; Berezin M. Y. Design of irreversible optical nanothermometers for thermal ablations. *Chem. Commun.* **2013**, *49*, 680-682.

- (16) Ito, E; Kang, H; Lee, D; Park, J. B.; Hara, M.; Noh, J. Spontaneous desorption and phase transitions of self-assembled alkanethiol and alicyclic thiol monolayers chemisorbed on Au(1 1 1) in ultrahigh vacuum at room temperature. *J. Colloid Interface Sci.* **2013**, *394*, 522-529.
- (17) Bain, C. D.; Troughton, E. B.; Tao, Y.-T.; Evall, J.; Whitesides, G. M.; Nuzzo, R. G. Formation of Monolayer Films by the Spontaneous Assembly of Organic Thiols from Solution onto Gold. *J. Am. Chem. Soc.* **1989**, *111*, 321-335.
- (18) Maciel, J.; Martins, M. C. L.; Barbosa, M. A. The stability of self-assembled monolayers with time and under biological conditions. *J. Biomed. Mater. Res., Part A* **2010**, *94A*, 833-843.
- (19) Mani, G.; Johnson, D. M.; Marton, D.; Dougherty, V. L.; Feldman, M. D.; Patel, D.; Ayon, A. A.; Agrawal, C. M. Stability of self-assembled monolayers on titanium and gold. *Langmuir* **2008**, *24*, 6774–6784.
- (20) Hostetler, M. J.; Templeton, A. C.; Murray, R. W.; Dynamics of place-exchange reactions on monolayer-protected gold cluster molecules. *Langmuir* **1999**, *15*, 3782-3789.
- (21) Song, Y.; Murray, R. W. Dynamics and extent of ligand exchange depend on electronic charge of metal nanoparticles. *J. Am. Chem. Soc.* **2002**, *124*, 7096-7102.
- (22) Haller, E.; Stubiger, G.; Lafitte, D.; Lindner, W.; Lammerhofer, M. Chemical Recognition of Oxidation-Specific Epitopes in Low-Density Lipoproteins by a Nanoparticle Based Concept for Trapping, Enrichment, and Liquid Chromatography–Tandem Mass Spectrometry Analysis of Oxidative Stress Biomarkers. *Anal. Chem.* **2013**, *49*, 680-682.
- (23) Bhatt, N.; Huang, P. J.; Dave, N.; Liu, J. Dissociation and degradation of thiol-modified DNA on gold nanoparticles in aqueous and organic solvents. *Langmuir* **2011**, *27*, 6132-6137.
- (24) Zandberg, W. F.; Bakhtiari, A. B. S.; Erno, Z.; Hsiao, D.; Gates, B. D.; Claydon, T.; Branda, N. R.; Photothermal release of small molecules from gold nanoparticles in live cells. *Nanomed. Nanotech. Biol. Med.* **2012**, *8*, 908–915.

- (25) Rahme, K.; Chen, L.; Hobbs, R. G.; Morris, M. A.; O'Driscoll, C.; Holmes, J. D. PEGylated gold nanoparticles: polymer quantification as a function of PEG lengths and nanoparticles dimensions. *RCS Adv.* **2013**, *3*, 6085-6094.
- (26) Manson, J.; Kumar, D.; Meenan, B. J.; Dixon, D. Polyethylene glycol functionalized gold nanoparticles: the influence of capping density on stability in various media. *Gold Bull.* **2011**, *44*, 99-105.
- (27) Kumar, R.; Korideck, H.; Ngwa, W.; Berbeco, R. I.; Makrigiorgos, G. M.; Sridhar, S. Third generation gold nanoplatfrom optimized for radiation therapy. *Transl. Cancer Res.* **2013**, *4*, 228-239.
- (28) Shenoi, M. M.; Iltis, I.; Jeunghwan, C.; Koonce, N. A.; Metzger, G. J.; Griffin, R. J.; Bischof, J. C. Nanoparticles delivered vascular distributing agents (VDAs): Use of TNF-alpha conjugated gold nanoparticles for multimodal cancer therapy. *Mol. Pharmaceutics* **2013**, *10*, 1683-1694.
- (29) Oishi, M.; Nakamura, T.; Jinji, Y.; Matsuishi, K.; Nagasaki, Y. Multi-stimuli-triggered release of charged dye from smart PEGylated nanogels containing gold nanoparticles to regulate fluorescence signals. *J. Mater. Chem.* **2009**, *19*, 5909-5912.
- (30) Sironi, L.; Freddi, S.; D'Alfonso, L.; Collini, M.; Gorletta, T.; Soddu, S.; Chirico, G. Detection by fluorescence lifetime on a hybrid fluorescein isothiocyanate gold nanosensor. *J. Biomed. Nanotechnol.* **2009**, *5*, 683-691.
- (31) Zhang, J.; Lio, B.; Liu, H.; Zhang, X.; Tan, W. Aptamer – conjugated gold nanoparticles for bioanalysis. *Nanomedicine* **2013**, *8*, 983-993.
- (32) Huff, T. B.; Tong, L.; Zhao, Y.; Hansen, M. N.; Cheng, J. X.; Wei, A. Hyperthermic effects of gold nanorods on tumor cells. *Nanomedicine* **2007**, *2*, 125–132.
- (33) Freddi, S.; Sironi, L.; D'Antuono, R.; Morone, D.; Donà, A.; Cabrini, E.; D'Alfonso, L.; Collini, M.; Pallavicini, P.; Baldi, G.; Maggioni, D.; Chirico, G. A molecular thermometer for nanoparticles for optical hyperthermia. *Nanoletters* **2013**, *13*, 2004-2010.

- (34) Casu, A.; Cabrini, E.; Donà, A.; Falqui, A.; Diaz-Fernandez, Y.; Milanese, C.; Taglietti, A.; Pallavicini, P. Controlled synthesis of gold nanostars using a zwitterionic surfactant. *Chem. - Eur. J.* **2012**, *18*, 9381-9390.
- (35) Yuan, H.; Fales, A. M.; Vo-Dinh, T. TAT Peptide-Functionalized Gold Nanostars: Enhanced Intracellular Delivery and Efficient NIR Photothermal Therapy Using Ultralow Irradiance. *J. Am. Chem. Soc.* **2012**, *134*, 11358–11361.
- (36) Pallavicini, P.; Donà, A.; Taglietti, A.; Minzioni, P.; Patrini, M.; Dacarro, G.; Chirico, G.; Sironi, L.; Bloise, N.; Visai, L.; Scarabelli, L. Self-assembled monolayers of gold nanostars: a convenient tool for near-IR photothermal biofilm eradication. *Chem. Commun.* **2014**, *50*, 1969-1971.
- (37) Voliani, V.; Signore, G.; Nifosi, R.; Rici, F.; Luin, S.; Beltram, F. Smart delivery and controlled drug release with gold nanoparticles: new frontiers in nanomedicine. *Recent Pat. Nanomed.* **2012**, *2*, 34-44.
- (38) Yang, P. J.; Chu, H.; Lee, Y.; Kobayashi, T.; Chen, T.; Ling, H. Quenching effects of gold nanoparticles in nanocomposites formed in water-soluble conjugated polymer nanoreactors. *Polymer* **2012**, *53*, 239-946.
- (39) Dulkeith, E.; Ringler, M.; Klar, T. A.; Feldmann, J.; Javier, A. M.; Parak, W. J. Gold nanoparticles quench fluorescence by phase induced radiative rate suppression. *Nano Letters* **2005**, *5*, 585-589.
- (40) Anger, P.; Bharadwaj, P.; Novotny, L. Enhancement and quenching of single-molecule fluorescence. *Phys. Rev. Lett.* **2006**, *96*, 113002.
- (41) Thivierge, C.; Bandichhor, R.; Burgess, K. Spectral dispersion and water solubilization of Bodipy dyes via palladium catalyzed C-H functionalization. *Org. Lett.* **2007**, *9*, 2135-2138.
- (42) Pallavicini, P.; Bernhard, C.; Dacarro, G.; Denat, F.; Diaz-Fernandez, Y.; Goze, C.; Pasotti, L.; Taglietti, A. Optical method for predicting the composition of self-assembled monolayers of mixed thiols on surfaces coated with silver nanoparticles. *Langmuir* **2012**, *28*, 3558-3568.

- (43) Kumar, D.; Meenan, J. B.; Dixon, D. Glutathione-mediated release of Bodipy from PEG cofunctionalized gold nanoparticles. *Int. J. Nanomed.* **2012**, *7*, 4007-4022.
- (44) Kumar, D.; Mutreja, I.; Meenan, J. B.; Dixon, D. Profile of polyload release from gold nanoparticles modified with Bodipy/PEG mixed monolayer. *Journal of Nano Research* **2013**, *25*, 16-30.
- (45) Peng, H.; Chen, W.; Cheng, Y.; Hakuna, L.; Strongin, R.; Wang, B. Thiol reactive probes and chemosensors. *Sensors* **2012**, *12*, 15907-15946.
- (46) Nagai, A.; Yoshii, R.; Otsuka, T.; Kokado, K.; Chujo, Y. Bodipy-based chain transfer agent: reversibly thermoswitchable luminescent gold nanoparticles stabilized by Bodipy-terminated water-soluble polymer. *Langmuir* **2010**, *26*, 15644-15649.
- (47) Theillet, F.-X.; Binolfi, A.; Fremdgen-Kesner, T.; Hingorani, K.; Sarkar, M.; Kyne, C.; Conggang, L.; Crowley, P. B.; Gierasch, L.; Pielak, G. J.; Elcock, A. H.; Gershenson, A.; Selenko, P. Physicochemical properties of cells and their effects on intrinsically disordered proteins (IDPs). *Chem Rev.* **2014**, *114*, 6661-6714.
- (48) Lee, E. S.; Bae, Y. H. Recent progress in tumor pH targeting nanotechnology. *J. Controlled Release* **2008**, *132*, 164-170.
- (49) Chirico, G.; Beretta, S.; Baldini, G. Conformation of interacting lysozyme by polarized and depolarized light scattering. *J. Chem. Phys.* **1999**, *110*, 2297-2304.
- (50) Tanaka, T. *Experimental methods in polymer science*. Academic Press: London, 2000.
- (51) Wang, Y.; Kuenzer, C. On gradient methods for maximum entropy regularizing retrieval of atmospheric aerosol particle distribution function. *Proc. Appl. Math. Mech.* **2007**, *7*, 1042103-1042104.
- (52) Lévy, R.; Thanh, N. T. K.; Doty, R. C.; Hussain, I.; Nichols, R. J.; Schiffrin, D. J.; Brust, M.; Fernig, D. G. Rational and Combinatorial Design of Peptide Capping Ligands for Gold Nanoparticles. *J. Am. Chem. Soc.* **2004**, *126*, 10076-10084.

- (53) Pallavicini, P. Bernhard, C. Chirico, G. Dacarro, G. Denat, F. Donà, A. Milanese, C. Taglietti, A. Gold nanostars co-coated with the Cu(II) complex of a tetraazamacrocyclic ligand. *Dalton Trans.* **2015**, 44, 5652-5561.
- (54) Montalti, M.; Prodi, L.; Zaccheroni, N.; Battistini, G. Modulation of the photophysical properties of gold nanoparticles by accurate control of the surface coverage. *Langmuir* **2004**, 18, 7884-7886.
- (55) Bain, C. D.; Whitesides, G. M. Formation of two-component surfaces by the spontaneous assembly of monolayers on gold from solutions containing mixtures of organic thiols. *J. Am. Chem. Soc.* **1988**, 110, 6560-6561.
- (56) Bain, C. D.; Whitesides, G. M. Formation of monolayers by the coadsorption of thiols on gold: variation in the length of the alkyl chain. *J. Am. Chem. Soc.* **1989**, 111, 7164-7175.
- (57) Laibinis, P. E.; Fox, M. A.; Folkers, J. P.; Whitesides, G. M. Comparison of self-assembled monolayers on silver and gold – mixed monolayers derived from HS(CH₂)₂₁X and HS(CH₂)₁₀Y (X,Y= CH₃, CH₂OH) have similar properties. *Langmuir* **1991**, 7, 3167–3173.
- (58) Rumyantsev, E. V.; Alyoshin, S. N.; Martin, Y. S. Kinetic study of Bodipy resistance to acids and alkalis: Stability ranges in aqueous and non-aqueous solutions. *Inorg. Chim. Acta* **2013**, 408, 181-185.
- (59) Sironi, L.; Freddi, S.; Caccia, M.; Pozzi, P.; Rosetti, L.; Pallavicini, P.; Donà, A.; Cabrini, E.; Gualtieri, M.; Rivolta, I.; Panariti, A.; D'Alfonso, L.; Collini, M.; Chirico, G. Gold branched nanoparticles for cellular treatments. *J. Phys. Chem. C*, **2012**, 116, 18407-18418.
- (60) Cavallaro, G.; Triolo, D.; Licciardi, M.; Giammona, G.; Chirico, G.; Sironi, L.; Dacarro, G.; Donà, A.; Milanese, C.; Pallavicini, P. Amphiphilic Copolymers Based on Poly[(hydroxyethyl)-D,L-aspartamide]: A Suitable Functional Coating for Biocompatible Gold Nanostars. *Biomacromolecules* **2013**, 14, 4260–4270.

TOC graphic

